CWP-598

Elastic wavefield separation for VTI media

Jia Yan and Paul Sava
Center for Wave Phenomena, Colorado School of Mines

ABSTRACT
The separation of wave modes from isotropic elastic wavefields is typically done using Helmholtz decomposition. However, Helmholtz decomposition using conventional divergence and curl operators in anisotropic media does not give satisfactory results and leaves the different wave modes only partially separated. The separation of anisotropic wavefields requires the use of more sophisticated operators which depend on local material parameters. We construct operators for anisotropic wavefield separation based on the polarization vectors evaluated at each point of the medium by solving the Christoffel equation using local medium parameters. These polarization vectors can be represented in the space domain as localized convolutional operators, which resemble conventional derivative operators. The spatially-variable "pseudo " derivative operators perform well in heterogeneous VTI media even at places where the media are changing rapidly. Synthetic results indicate that the operators can be used to separate wavefields for VTI media with arbitrary degree of anisotropy. This methodology is applicable for elastic reverse time migration (RTM) in heterogeneous anisotropic media.

Key words: elastic, imaging, anisotropic

1 INTRODUCTION

Wave equation migration for elastic data usually consists of two steps. The first step is wavefield reconstruction in the subsurface from data recorded at the surface. The second step is an imaging condition which extracts reflectivity information from the reconstructed wavefields.

The elastic wave equation migration can be implemented in two ways. The first approach is to separate recorded elastic data into compressional and transverse (P and S) modes, and use these separated modes for acoustic wave equation migration respectively. This acoustic imaging approach to elastic waves is more frequently done, but it is based on the assumption that P and S data can be successfully separated on the surface, which is not always true (Etgen, 1988; Zhe & Greenhalgh, 1997). The second approach is to not separate P and S modes on the surface, extrapolate the entire elastic wavefield at once, then separate wave the modes prior to applying an imaging condition. The reconstruction of elastic wavefields can be implemented using various techniques, including reconstruction by time reversal (RTM) (Chang & McMechan, 1986, 1994) or by Kirchhoff integral techniques (Hokstad, 2000). The imaging condition (I.C.) applied to the reconstructed vector wavefields directly determines the quality of the images. Conventional cross-correlation imaging condition does not separate the wave modes and cross-correlates the Cartesian components of the elastic wave components. In general, the various wave modes (P and S) are mixed on all wavefield components, and cause crosstalk and image artifacts. Yan & Sava (2007) suggest using imaging conditions based on elastic potentials, which require cross-correlation of separated modes. Potential-based imaging condition creates images that have clear physical meanings, in contrast with images obtained with wavefield components, thus justifying the need for wave mode separation.

As the need for anisotropic imaging increases, more and more processing and migration are performed based on anisotropic acoustic one-way wave equations (Alkhalifah, 1998; Shan, 2006; Shan & Biondi, 2005). However, much less research has been done on anisotropic elastic migration based on two-way wave equations. Elastic Kirchhoff migration (Hokstad, 2000) obtains pure-mode and converted mode images by downward continuation of elastic vector wavefields with a visco-elastic wave equation. The wavefield separation is effectively done with elastic Kirchhoff integration, which handles both P- and S-waves. However, Kirchhoff migration does no perform well in areas of complex geology where ray theory breaks down (Gray *et al.*, 2001), thus requiring migration with more accurate methods, e.g., reverse time migration.

One of the complexities that impedes elastic wave equa-

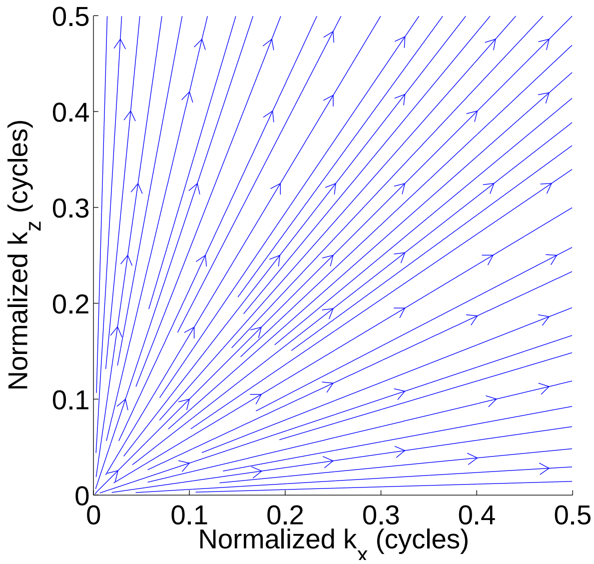

(a)

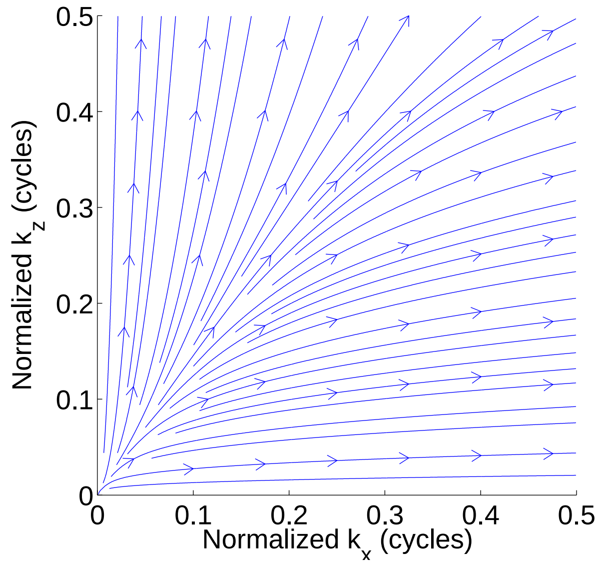

(b)

Figure 1. The polarization vectors as a function of wavenumbers k_x and k_z for (a) an isotropic model with $V_P = 3$ km/s and $V_S = 1.5$ km/s, and (b) an anisotropic (VTI) model with $V_{P0} = 3$ km/s, $V_{S0} = 1.5$ km/s, $\epsilon = 0.25$ and $\delta = -0.29$.

tion anisotropic migration is the difficulty to separate anisotropic wavefields into different wave modes. However, the proper separation of anisotropic wave modes is as important for anisotropic elastic migration as is the separation of isotropic wave modes for isotropic elastic migration. The main difference between anisotropic and isotropic wavefield separation is that Helmholtz decomposition is only suitable for the separation of isotropic wavefields, and does not work well for anisotropic wavefields.

In this abstract, we show how to construct wavefield separators for VTI (vertical transverse isotropy) media applicable to medels with spatially varying parameters. We apply these operators to anisotropic elastic wavefields and show that they successfully separate anisotropic wave modes, even for extremely anisotropic media.

2 SEPARATION METHOD

Separation of scalar and vector potentials can be achieved by Helmholtz decomposition, which is applicable to any vector field $\mathbf{W}(x, y, z)$. By definition, the vector wavefield $\mathbf{W}$ can be decomposed into a curl-free scalar potential Θ and a divergence-free vector potential $\mathbf{\Psi}$ according to the relation:

$$\mathbf{W} = \nabla\Theta + \nabla \times \mathbf{\Psi} . \tag{1}$$

Equation 1 is not used directly in practice, but the scalar and vector components are obtained indirectly by the application of the $\nabla \cdot$ and $\nabla \times$ operators to the extrapolated elastic wavefield:

$$P = \nabla \cdot \mathbf{W} , \tag{2}$$
$$\mathbf{S} = \nabla \times \mathbf{W} . \tag{3}$$

For isotropic elastic fields far from the source, quantities P and $\mathbf{S}$ describe compressional and transverse wave modes, respectively (Aki & Richards, 2002).

Equations 2 and 3 allows us to understand why $\nabla \cdot$ and $\nabla \times$ pass compressional and transverse wave modes, respectively. In the space domain, we can write:

$$P = \nabla \cdot \mathbf{W} = D_x * W_x + D_y * W_y + D_z * W_z , \tag{4}$$

where D_x, D_y and D_z represent derivatives in x, y and z directions and $*$ represents spatial convolution. In the Fourier domain, we can represent the operators D_x, D_y and D_z by $i\,k_x$, $i\,k_y$ and $i\,k_z$, therefore, we can write an equivalent expression to equation 4 as:

$$P = i\,\mathbf{k} \cdot \widetilde{\mathbf{W}} = i\,k_x\,\widetilde{W}_x + i\,k_y\,\widetilde{W}_y + i\,k_z\,\widetilde{W}_z , \tag{5}$$

where $\mathbf{k} = \{k_x, k_y, k_z\}$ represents the wave vectors, and $\widetilde{\mathbf{W}}(k_x, k_y, k_z)$ is the 3D Fourier transform of the wavefield $\mathbf{W}(x, y, z)$. We see that in this domain, the operator $i\,\mathbf{k}$ essentially projects the wavefield $\widetilde{\mathbf{W}}$ onto the wave vector $\mathbf{k}$, which represents the polarization direction for P waves. Similarly, the operator $\nabla \times$ projects the wavefield onto the direction orthogonal to the wave vector $\mathbf{k}$, which represents the polarization direction for S waves (Dellinger & Etgen, 1990). For illustration, Figure 1(a) shows the polarization vectors of the P mode of an isotropic model as a function of normalized k_x and k_z ranging from 0 to 0.5 cycles. The polarization vectors are radial because P waves in an isotropic medium are polarized in the same directions as the wave vectors.

Dellinger & Etgen (1990) suggest the idea that wave mode separation can be extended to anisotropic media by projecting the wavefields onto the directions in which the P and S modes are polarized. This requires that we modify the wave

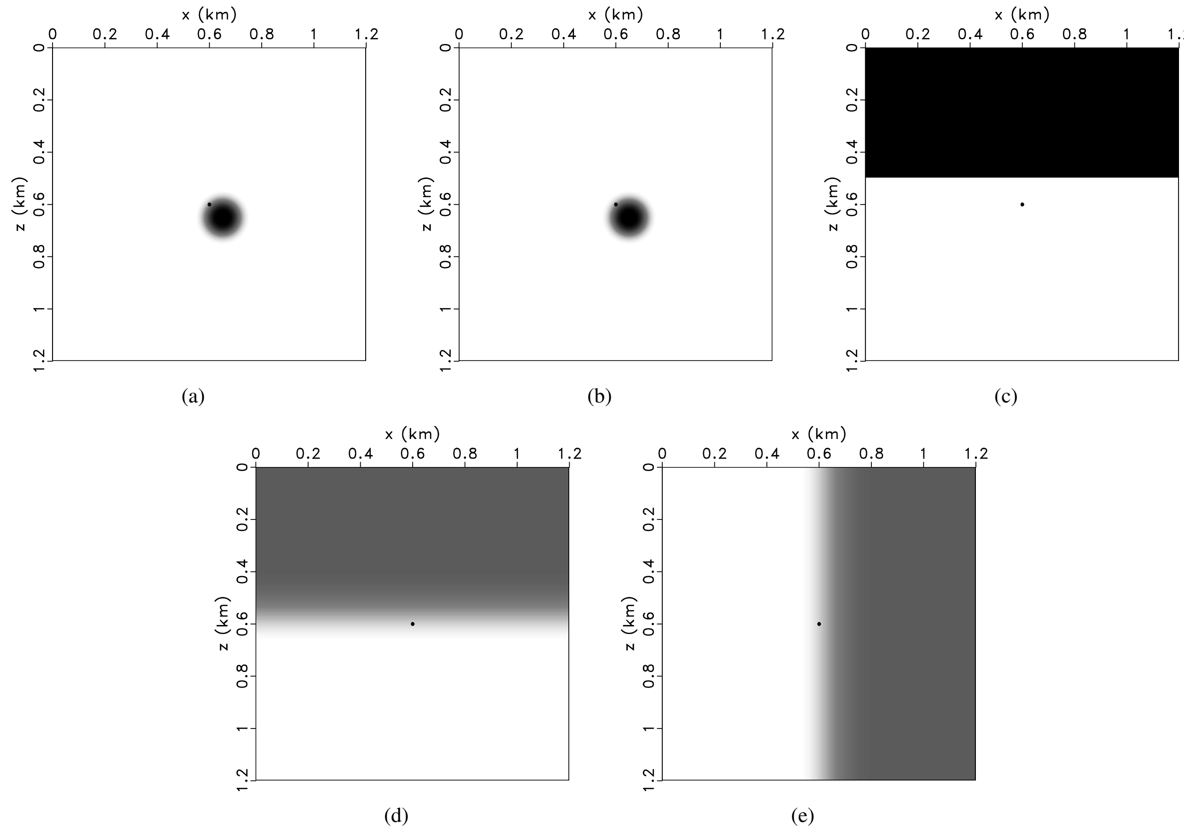

Figure 2. A 1.2 km$\times$ 1.2 km model that has parameters (a) $V_{p0} = 3$ km/s except for a low Gaussian anomaly at $x = 0.65$ km and $z = 0.65$ km, (b) $V_{S0} = 1.5$ km/s except for a low Gaussian anomaly at $x = 0.65$ km and $z = 0.65$ km, (c) $\rho = 1$ g/cm^3 in the top layer and 2 g/cm^3 in the bottom layer, (d) ϵ smoothly varying from 0 to 0.25 from top to bottom, (e) δ smoothly varying from 0 to -0.29 from left to right. The source is located at $x = 0.6$ km and $z = 0.6$ km.

separation equation 5 by projecting the wavefields onto the true polarization directions **U** to obtain *quasi*-P (*q*P) waves:

$$qP = i\,\mathbf{U}(\mathbf{k}) \cdot \widetilde{\mathbf{W}} = i\;U_x\;\widetilde{W}_x + i\;U_y\;\widetilde{W}_y + i\;U_z\;\widetilde{W}_z\,. \quad (6)$$

In anisotropic media, $\mathbf{U}(k_x, k_y, k_z)$ is different from **k**, as illustrated in Figure 1(b), which shows the polarization vectors of *q*P wave mode for an anisotropic model with normalized k_x and k_z ranging from 0 to 0.5 cycles. Polarization vectors are not radial because *q*P waves in an anisotropic medium are not polarized in the same directions as wave vectors, except in the symmetry planes ($k_z = 0$) and along the symmetry axis ($k_x = 0$).

We can write an equivalent expression to equation 6 in the space domain as:

$$qP = \nabla_a \cdot \mathbf{W} = L_x * W_x + L_y * W_y + L_z * W_z\,, \quad (7)$$

where L_x, L_y and L_z represent the inverse Fourier transforms of $i\,U_x$, $i\,U_y$ and $i\,U_z$, and $*$ represents spatial convolution. L_x, L_y and L_z define the pseudo derivative operators in x, y and z directions for an anisotropic medium, and they change from location to location according to the material parameters.

We obtain the polarization vectors $\mathbf{U}(\mathbf{k})$ by solving the Christoffel equation (Tsvankin, 2005):

$$\left[\mathbf{G} - \rho V^2 \mathbf{I}\right] \mathbf{U} = \mathit{0}\,, \quad (8)$$

where **G** is the Christoffel matrix $G_{ij} = c_{ijkl} n_j n_l$, in which c_{ijkl} is the stiffness tensor, n_j and n_l are the normalized wave vector components in the j and l directions, $i, j, k, l = 1, 2, 3$. V corresponds to the eigenvalues of the matrix **G**, which represent the phase velocities of each wave mode and are functions of k_x and k_z. In the symmetry planes of VTI media, equation 8 becomes

$$\begin{bmatrix} c_{11}k_x^2 + c_{55}k_z^2 - \rho V^2 & (c_{13} + c_{55})\,k_x k_z \\ (c_{13} + c_{55})\,k_x k_z & c_{55}k_x^2 + c_{33}k_z^2 - \rho V^2 \end{bmatrix} \begin{bmatrix} U_x \\ U_z \end{bmatrix} = 0\,, \quad (9)$$

which allows us to compute the components of the polarization vector **U** (the eigenvectors of the matrix **G**) of a given wave mode given the stiffness tensor and density at every location of the medium.

We can extend the procedure described in the preceding section to heterogeneous media by computing a different operator at every grid point. In the symmetry planes of VTI media, the operators are 2D and depend on the local values of the stiffness coefficients. For each point, we pre-compute

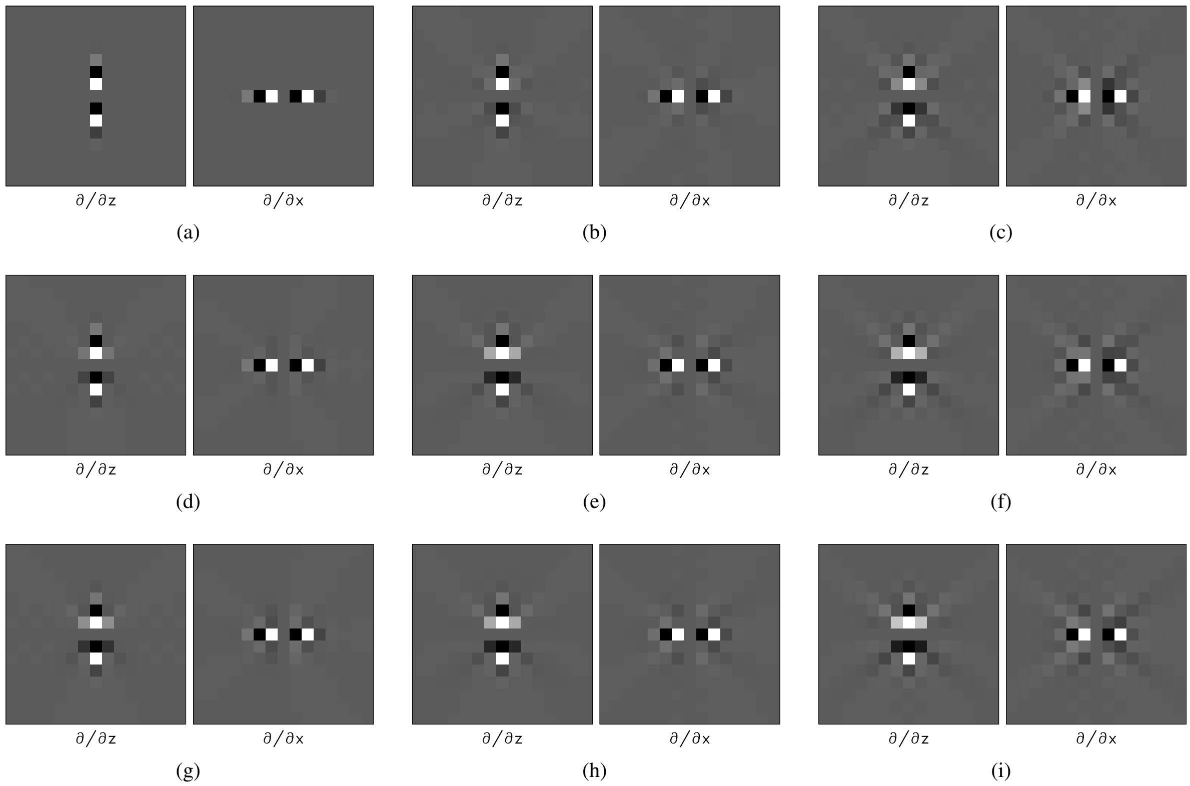

Figure 3. The 8^{th} order anisotropic pseudo derivative operators in the z and x directions at the intersections of x=0.3, 0.6, 0.9 km and z=0.3, 0.6, 0.9 km.

the polarization vectors as a function of the local medium parameters, and transform them to the space domain to obtain the wave mode separators. If we represent the stiffness coefficients using Thomsen parameters (Thomsen, 1986), then the pseudo derivative operators L_x and L_z depend on ϵ, δ, V_{P0} and V_{S0}, which are in general spatially dependent parameters. We can compute and store the operators for each grid point in the medium, and then use those operators to separate P and S modes from reconstructed elastic wavefields. Thus, wavefield separation in VTI media can be achieved simply by nonstationary convolution with operators L_x and L_z.

3 EXAMPLES

We consider a 2D isotropic model characterized by the V_P, V_S and density shown in Figures 2(a)–2(c). The model contains negative P and S velocity anomalies that triplicate the wavefields. The source is located in the center of the model. Figure 4(a) shows the vertical and horizontal components of the simulated elastic data, Figure 4(b) shows the separation to P and S modes using $\nabla\cdot$ and $\nabla\times$ operators, and Figure 4(c) shows the mode separation obtained using the pseudo operators dependent on the medium parameters. A comparison of Figures 4(b) and 4(c) indicates that the $\nabla\cdot$ and $\nabla\times$ operators and the pseudo operators work identically well for isotropic media.

We consider a 2D anisotropic model analogous to the one described by the parameters shown in Figures 2(a)–2(c) (with V_P, V_S representing the vertical P and S wave velocities), and additionally characterized by the parameters ϵ and δ shown in Figures 2(d) and 2(e). The parameters ϵ and δ vary gradually from top to bottom and left to right, respectively. The upper left part of the medium is isotropic and the lower right part is highly anisotropic. Since the difference of ϵ and δ is large at the bottom part of the model, the S waves in that region are severely triplicated due to this strong anisotropy.

Figure 3 illustrates the pseudo derivative operators obtained at different locations in the model defined by the intersections of x coordinates 0.3, 0.6, 0.9 km and z coordinates 0.3, 0.6, 0.9 km. Since the operators correspond to different combination of the parameters ϵ and δ, they have different forms. The isotropic operators are purely vertical and horizontal, while the anisotropic operators have tails radiating from the center.

Figure 5(a) shows the vertical and horizontal components of the simulated elastic anisotropic data, Figure 5(b) shows the separation to P and S modes using conventional $\nabla\cdot$ and $\nabla\times$ operators, and Figure 5(c) shows the mode separation obtained using the pseudo operators constructed using the local medium parameters. A comparison of Figure 4(b) and 4(c) in-

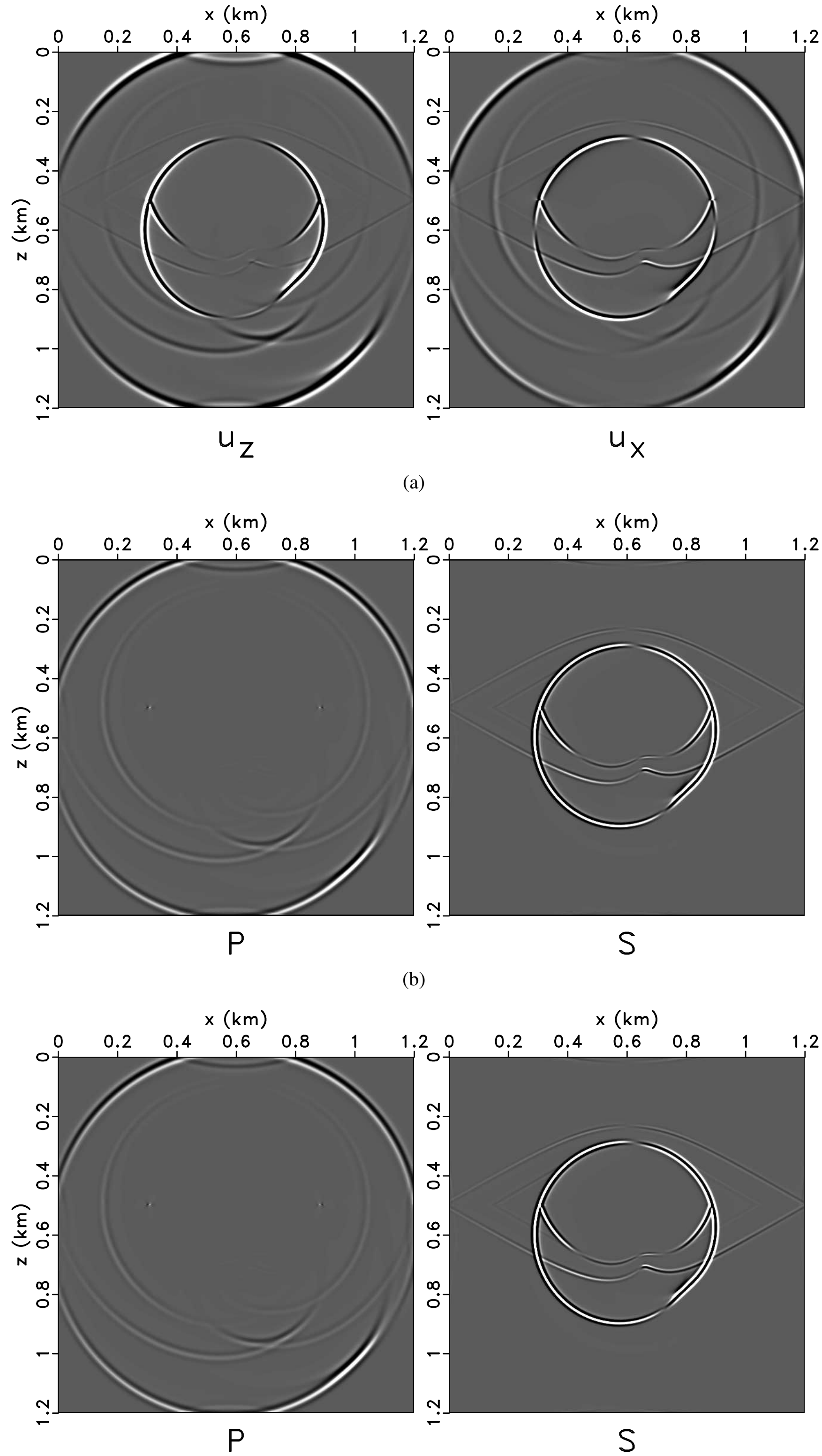

Figure 4. (a) Isotropic wavefield modeled with a vertical source at x=0.6 km and z=0.6 km, isotropic wave modes separated by (b) $\nabla \cdot$ and $\nabla \times$ and (c) pseudo derivative operators.

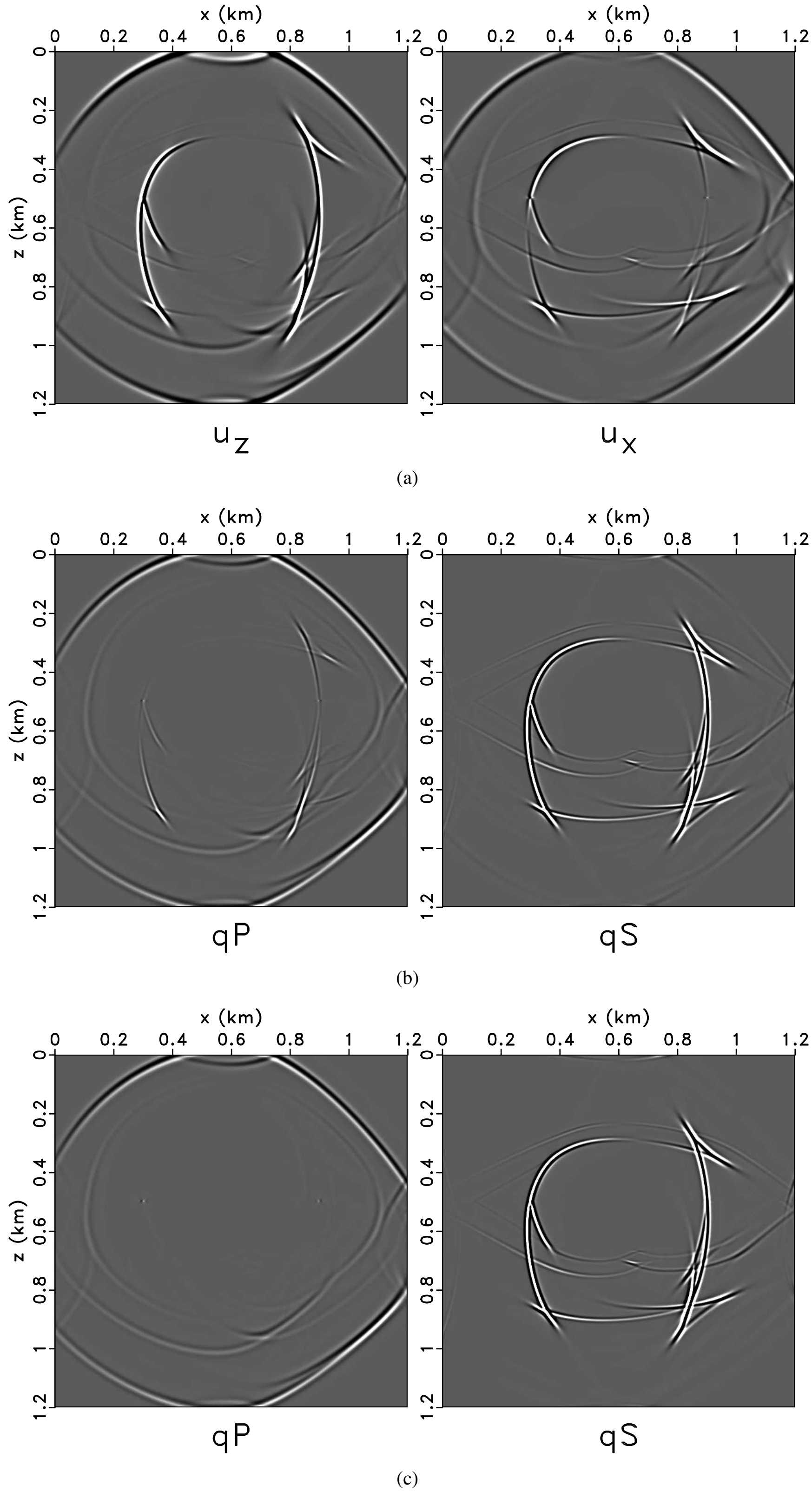

Figure 5. (a) Anisotropic wavefield modeled with a vertical source at x=0.6 km and z=0.6 km, anisotropic wave modes separated by (b) $\nabla \cdot$ and $\nabla \times$ and (c) pseudo derivative operators.

dicates that the spatially-varying derivative operators successfully separate the elastic wavefields into P and S modes, while $\nabla \cdot$ and $\nabla \times$ only work in the isotropic region of the model.

4 CONCLUSIONS

We present a method of obtaining spatially-varying pseudo derivative operators with application to wave mode separation in anisotropic media. The main idea is to utilize polarization vectors constructed in the wavenumber domain using the local media parameters at specific locations and then transform back to the space domain. The main advantage of applying the pseudo derivative operators in the space domain is that they can be used for heterogeneous media. The wave mode separators obtained using the method described in this abstract are spatially-variable convolutional operators and can be used to separate wavefields in VTI media with arbitrary degree of anisotropy. This methodology is applicable for elastic RTM in heterogeneous anisotropic media.

ACKNOWLEDGMENT

We acknowledge the support of the sponsors of the Consortium Project at the Center for Wave Phenomena at Colorado School of Mines.

REFERENCES

Aki, K., and Richards, P., 2002, Quantitative seismology (second edition): , University Science Books.

Alkhalifah, T., 1998, Acoustic approximations for processing in transversely isotropic media: Geophysics, **63**, no. 2, 623–631.

Chang, W.-F., and McMechan, G. A., 1986, Reverse-time migration of offset vertical seismic profiling data using the excitation-time imaging condition: Geophysics, **51**, no. 1, 67–84.

Chang, W.-F., and McMechan, G. A., 1994, 3-D elastic prestack, reverse-time depth migration: Geophysics, **59**, no. 4, 597–609.

Dellinger, J., and Etgen, J., 1990, Wave-field separation in two-dimensional anisotropic media (short note): Geophysics, **55**, no. 07, 914–919.

Etgen, J. T., 1988, Prestacked migration of P and SV-waves: SEG Technical Program Expanded Abstracts, **7**, no. 1, 972–975.

Gray, S. H., Etgen, J., Dellinger, J., and Whitmore, D., 2001, Seismic migration problems and solutions: Geophysics, **66**, no. 5, 1622–1640.

Hokstad, K., 2000, Multicomponent Kirchhoff migration: Geophysics, **65**, no. 3, 861–873.

Shan, G., and Biondi, B., 2005, 3D wavefield extrapolation in laterally-varying tilted ti media: SEG Technical Program Expanded Abstracts, **24**, no. 1, 104–107.

Shan, G., 2006, Optimized implicit finite-difference migration for VTI media: SEG Technical Program Expanded Abstracts, **25**, no. 1, 2367–2371.

Thomsen, L., 1986, Weak elastic anisotropy: Geophysics, **51**, no. 10, 1954–1966.

Tsvankin, I., 2005, Seismic signatures and analysis of reflection data in anisotropic media: 2nd edition: , Elsevier Science Publ. Co., Inc.

Yan, J., and Sava, P., 2007, Elastic wavefield imaging with scalar and vector potentials: SEG Technical Program Expanded Abstracts, **26**, no. 1, 2150–2154.

Zhe, J., and Greenhalgh, S. A., 1997, Prestack multicomponent migration: Geophysics, **62**, no. 02, 598–613.